Professional paper

Informacije MIDEM
Journal of Microelectronics,
Electronic Components and Materials
Vol. 45, No. 1 (2015), 80 – 86

A Study of Analytical Solutions of Plate Equation for Pressure Microsensor Diaphragm: Limitations, Comparison and Usage

S. Santosh Kumar[1,2] and B. D. Pant[1,2]

[1]CSIR–Central Electronics Engineering Research Institute (CEERI), Pilani, Rajasthan, India
[2]Academy of Scientific and Innovative Research (AcSIR), New Delhi, India

Abstract: Analytical solutions of plate equation for square diaphragms provide quick estimation of the output characteristics of pressure sensors before finite element method (FEM) analysis. In this work, we analyze the limitations of using the model of a plate for the diaphragm of a piezoresistive pressure sensor. A comparison of various solutions of plate equations available in literature with FEM solution of plate is also carried out. Based on the above analysis, the most accurate analytical solution is determined. Using this solution, the methodology of obtaining the sensitivity and non-linearity of piezoresistive pressure sensors is delineated. This study shows the scope and limitations of using analytical solutions of plate equations for obtaining the output characteristics of a pressure sensor.

Keywords: Analytical equations; finite element method (FEM); piezoresistive pressure sensors

Študija analitične rešitve enačbe plošče za mikrosenzorsko tlačno opno: omejitve, primerjava in uporaba

Izvleček: Analitične rešitve enačbe plošče za kvadratno opno predstavljajo hitro ocenitev izhodnih karakteristik senzorjev tlaka še pred analizo z metodo končnih elementov (FEM). V delu predstavljamo omejitve uporabljene metode na opni piezorezistivnega senzorja tlaka. Opravljena je tudi primerjava različnih objavljenih rešitev enačbe plošče s FEM rešitvijo. Na osnovi te analize je določena najboljša rešitev, ki je uporabljena za določitev občutljivosti in nelinearnosti piezorezistivnega senzorja tlaka. Študija predstavlja omejitve uporabe metode za določevanje izhodnih karakteristik senzorja.

Ključne besede: analitične enačbe; metoda končnih elementov (FEM); piezorezistivni sensor tlaka

* *Corresponding Author's e-mail: santoshkumar.ceeri@gmail.com*

1 Introduction

Pressure sensors constitute a major portion of sales in the microelectromechanical systems (MEMS) mechanical sensors market [1]. Various transduction mechanisms are used in these sensors to convert the pressure input into an electrical signal. Based on these transduction mechanisms, pressure sensors can be classified as capacitive, piezoresistive, piezoelectric, optical and resonant [2, 3]. Piezoresistive pressure sensors have several advantages like small size, high linearity, high reliability and simple IC fabrication [4]. These sensors are used in applications like tire pressure monitoring system (TPMS), intracranial pressure measurement, aircraft gas turbine combustion control and chemical processing. Piezoresistive pressure sensors usually consist of four resistors (also known as piezoresistors), connected in a Wheatstone bridge arrangement, on top of a diaphragm. The diaphragm of a pressure sensor is formed by bulk micromachining of silicon using wet chemical etchants or dry etching using deep-reactive-ion-etching (DRIE). When the diaphragm of a sensor is stressed (under the influence of a pressure load), the resistance of the piezoresistors changes due to piezoresistivity. Thus, the output of the Wheatstone

bridge gives an estimate of the pressure input. In order to estimate the output characteristics of the sensor prior to fabrication, finite element method (FEM) based tools are used. However, analytical methods help in obtaining a quick estimate of the important output parameters like sensitivity and linearity before moving on to time consuming FEM based simulations [5, 6]. The diaphragm of a pressure sensor can be assumed to be a thin plate clamped at the edges. However, the above assumption has some flaws owing to the difference in the boundary condition in a plate and in an actual pressure sensor diaphragm as shown in Fig. 1. For square diaphragm based pressure sensors, no accurate solutions are available for plate equations. Over the years various approximate solutions have been proposed in the literature for the diaphragm deflection [6-10]. The diaphragm deflection is related with the surface stresses on the diaphragm and thus is related with the output of the sensor.

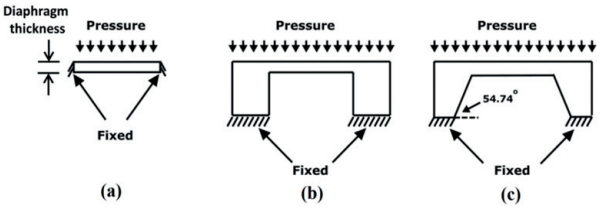

Figure 1: Cross-section and boundary conditions. (a) Plate. (b) Diaphragm etched using deep-reactive-ion-etching. (c) Diaphragm etched using wet bulk micromachining.

In this paper, we first analyze the effect of boundary conditions on deflection and stress on the diaphragm using FEM tools. Next, the accuracy of different analytical solutions of plate equations for square diaphragm available in literature is estimated by comparing them with FEM simulations of a plate. Finally, using the most accurate analytical solution, the methodology for obtaining sensitivity and linearity of the sensor is delineated.

2 Governing equations

The differential equation for a two dimensional square plate (as shown in Fig. 2) with a uniform pressure load, *P*, can be expressed as [11]:

$$D\left[\frac{\partial^4 w}{\partial x^4}+2\frac{\partial^4 w}{\partial x^2\partial y^2}+\frac{\partial^4 w}{\partial y^4}\right]=P \tag{1}$$

where $D = Eh^3/12(1-\nu^2)$ is the flexural rigidity of the diaphragm, and w is the deflection of the diaphragm at (x,y). *E* is the Young's modulus of silicon, *h* is the thickness of the diaphragm, and **v** is the Poisson's ratio of silicon.

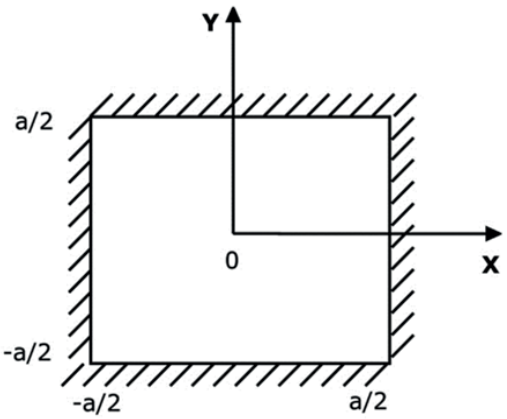

Figure 2: Schematic of a square plate.

The boundary conditions for the plate shown in Fig. 2 are as follows:

$$W\left(x=\pm\frac{a}{2};y\right)=0 \tag{2}$$

$$W\left(x;y=\pm\frac{a}{2}\right)=0 \tag{3}$$

$$\frac{\partial w}{\partial x}\left(x=\pm\frac{a}{2};y\right)=0 \tag{4}$$

$$\frac{\partial w}{\partial y}\left(x;y=\pm\frac{a}{2}\right)=0 \tag{5}$$

The solution of Eq. (1) with the above boundary conditions yields an expression for *w*(x,y). This expression can then be plugged into Eq. (6) and Eq. (7) to obtain the surface stresses of the diaphragm.

$$\sigma_x=-\frac{Eh}{2(1-\nu^2)}\left(\frac{\partial^2 w}{\partial x^2}+\nu\frac{\partial^2 w}{\partial y^2}\right) \tag{6}$$

$$\sigma_y=-\frac{Eh}{2(1-\nu^2)}\left(\frac{\partial^2 w}{\partial y^2}+\nu\frac{\partial^2 w}{\partial x^2}\right) \tag{7}$$

where $\boldsymbol{\sigma}_x$ and $\boldsymbol{\sigma}_y$ are the x- and y-directed surface stresses, respectively. In the above equations, it is assumed that the diaphragm bending is elastic and the diaphragm deflection is small compared to diaphragm thickness (less than 1/5th of the diaphragm thickness).

3 Effect of clamping conditions

The clamping conditions used in a plate rigidly clamped at all the four edges (Fig. 1 (a)) are different from those

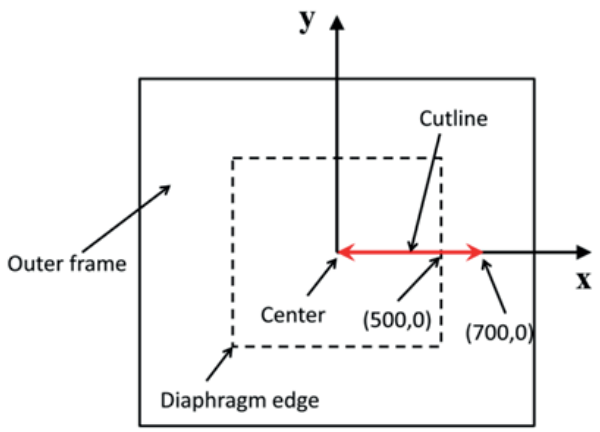

Figure 3: Top view of cutline along x-axis.

found in actual pressure sensor fabricated using DRIE and Wet bulk micromachining (WBM) as shown in Fig. 1 (b) and 1 (c), respectively. This boundary condition affects the magnitude of stress and the stress distribution on the top surface of the diaphragm where the piezoresistors are placed. In order to determine the effect of this boundary condition on the stress distribution, the x-direction stress for the three models (as shown in Fig. 1 (a)–(c)) are compared using FEM tool Coventorware. A square diaphragm of size 1000 µm x 1000 µm is used in the simulations. Simulations are performed for diaphragm thicknesses of 30 µm, 40 µm, 50 µm and 60 µm. A pressure load of 10 Bar is applied on all the diaphragms for these simulations. The x-directed stress along the cutline as shown in Fig. 3 is determined using these simulations. Fig. 4 shows the result of these simulations. It is clear from the result that the stress distribution is dependent upon the clamping conditions used for the simulations. In the DRIE and WBM model, the stress extends beyond the edge of the diaphragm (at x = 500 µm). The DRIE and WBM model show stress values close to each other in all the cases. However, it

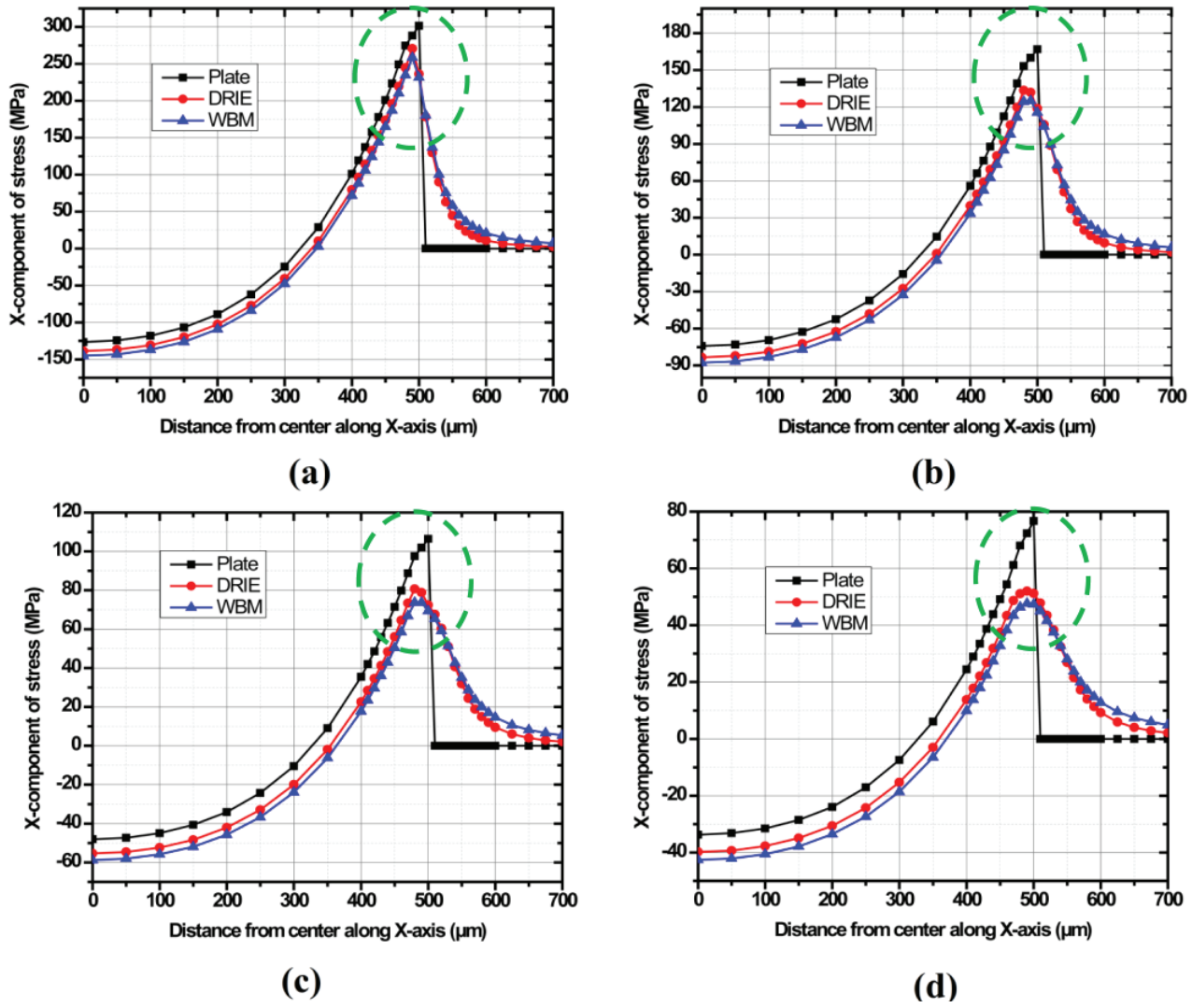

Figure 4: X-directed stress along cutline in diaphragm with different thicknesses. (a) 30 µm. (b) 40 µm. (c) 50 µm. (d) 60 µm.

can be observed that as the thickness of the diaphragm increases, the stresses near the edge of the diaphragm for the plate model is farther away from other models (as shown in the region encircled by dotted lines). This indicates that the diaphragm in a pressure sensor can be approximated by the plate model only for thin diaphragms and the plate equations can be used in such a situation. Also, the piezoresistors cannot be placed outside the diaphragm edges when plate equations are used to analyze the diaphragm as the stress fields outside the diaphragm edges cannot be evaluated. Thin diaphragms are more sensitive and less linear and the vice versa is true for thick diaphragms. For good sensitivity and linearity, diaphragm must neither be too thick nor too thin. Analytical solutions of plate equations provide sufficiently accurate solutions in this regime as they are valid in such cases.

4 Comparison of different solutions for plate equation with FEM

For the square diaphragm, many approximate solutions are available in literature. These define the deflection (*w*) of the diaphragm at a given (x,y). Some of these solutions are [6-8]:

$$w = 0.0213P\frac{a^4}{16D}\left(1-\frac{4x^2}{a^2}\right)^2\left(1-\frac{4y^2}{a^2}\right)^2 \tag{8}$$

$$w = \frac{w_0}{4}\left[1+\cos\left(\frac{2\pi\ \mathrm{x}}{\mathrm{a}}\right)\right]\left[1+\cos\left(\frac{2\pi\ \mathrm{y}}{\mathrm{a}}\right)\right] \text{where}$$

$$\frac{P\left(\frac{a}{2}\right)^4}{12C_bD}, \mathrm{C_b} = 4.06 \tag{9}$$

$$w = P\frac{a^4}{16D}\left(1-\frac{4x^2}{a^2}\right)^2\left(1-\frac{4y^2}{a^2}\right)^2 \left[0.02023+0.0214\frac{x^2+y^2}{a^2}+0.1\frac{x^2y^2}{a^4}\right] \tag{10}$$

$$w = \frac{49a^4b^4p}{8D\left(7b^4+4a^2b^2+7a^4\right)}\mathrm{x} \left(\frac{1}{2}-\frac{x}{a}\right)^2\left(\frac{1}{2}-\frac{y}{b}\right)^2\left(\frac{1}{2}+\frac{x}{a}\right)^2\left(\frac{1}{2}+\frac{y}{b}\right)^2 \tag{11}$$

Sometimes, a modified differential equation as shown in (12) is used for obtaining the solution of membrane on (100) plane with edges directed along <110> direction. This equation considers the anisotropic nature of the material properties of silicon.

$$\frac{\partial^4 w}{\partial x^4}+2\alpha\frac{\partial^4 w}{\partial x^2\partial y^2}+\frac{\partial^4 w}{\partial y^4}=\frac{P}{D} \tag{12}$$

where $\alpha = v+\frac{2G}{E}\left(1-v^2\right)$ is known as the anisotropy coefficient and characterizes the anisotropy in silicon. G is the shear modulus. For a square diaphragm, some of the proposed solutions for (12) are [9-10]:

$$w = \frac{0.02126\,a^2b^2p}{16D}\left[\left(1-\left(\frac{2x}{a}\right)^2\right)\left(1-\left(\frac{2y}{b}\right)^2\right)\right]^2\mathrm{x} \sum_{\mathrm{i=0}}^{\mathrm{n}}\sum_{\mathrm{j=0}}^{\mathrm{n}}k_{ij}\left(\frac{2x}{a}\right)^i\left(\frac{2y}{b}\right)^j \tag{13}$$

$$w = \frac{0.0224\,a^2b^2p}{16D}\sum_{\mathrm{i=0}}^{\mathrm{n}}\sum_{\mathrm{j=0}}^{\mathrm{n}}k_{ij}\cos^2\left(\frac{(2i+1)\pi\ x}{\mathrm{a}}\right)\mathrm{x} \cos^2\left(\frac{(2j+1)\pi\ y}{\mathrm{b}}\right) \tag{14}$$

where *n* is an even positive integer, *i*, *j* = 0,2,4,6,…..*n*, k_{ij} are the shape factors. The shape factors for n=4 is given in Table 1. In all the equations above, a = b, due to the diaphragm being square in shape.

Table 1: Shape factors for n = 4

	Eq. (13)	Eq. (14)
k_{00}	1	1
k_{20}	0.233	0.0284
k_{02}	0.233	0.0284
k_{22}	0.252	0.0123
k_{40}	-0.00166	0.0038
k_{04}	-0.00166	0.0038
k_{42}	0.13	0.0030
k_{24}	0.13	0.0030
k_{44}	-0.235	0.0016

The deflection of diaphragm obtained by the solutions of plate equations given by Eqs. (8), (9), (10), (11), (13), and (14) are compared with FEM solution in order to find the most accurate solution. A diaphragm size of 1000 µm × 1000 µm and diaphragm thickness of 30 µm are chosen for the comparative study. A pressure of 10 Bar is applied. Fig. 5 shows the combined plot of diaphragm deflection (along the x-axis) obtained using

different analytical equations. These solutions are compared with solution obtained using FEM. The material properties of silicon used in analytical solutions are as follows: Young's modulus (E) = 169.8 GPa and Poisson's ratio (v) = 0.066. Orthotropic properties of silicon are used in the FEM solution [12]. To find the most accurate solution, the root mean square deviation (RMSD) of each of the solution (from the FEM solution) is obtained using the following formula:

$$RMSD = \sqrt{\frac{\sum_{i=1}^{n}\left(Def_{i,Analytical} - Def_{i,FEM}\right)^2}{n}} \quad (15)$$

where n is the total number of points where the deflection is calculated on the cutline along x-axis, $Def_{i,analytical}$ is the diaphragm deflection obtained by the particular analytical solution at point *i*, $Def_{i,FEM}$ is the diaphragm deflection obtained by FEM solution at point *i*. The calculated value of RMSD is enlisted in Table 2.

Table 2: Root mean square deviation (RMSD) from FEM solution

Equation no.	RMSD
(8)	0.1994
(9)	0.2400
(10)	0.3906
(11)	0.2024
(13)	0.1414
(14)	0.1796

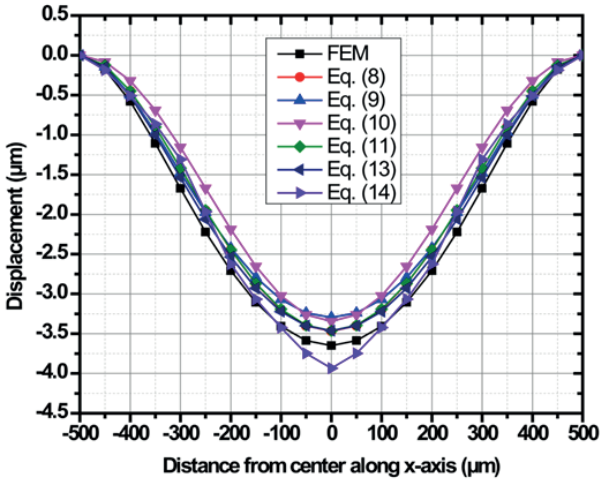

Figure 5: Comparison of diaphragm deflection obtained using different analytical solutions and FEM.

Table 2 indicates that the RMSD value obtained for Eq. (13) is the lowest. Hence, the solution given in Eq. (13) provides the most accurate picture of the diaphragm deflection for a plate and is chosen for calculating the output of the piezoresistive pressure sensor in next section.

5 Sensitivity and linearity calculations using analytical solution

Consider a pressure sensor diaphragm with four piezoresistors connected in Wheatstone bridge as shown in Fig. 6. The relative change in resistance of each resistor can be given by [13]:

$$\frac{\Delta R}{R} = \pi_l \sigma_l + \pi_t \sigma_t \quad (16)$$

where $\boldsymbol{\pi}_l$ and $\boldsymbol{\pi}_t$ are the longitudinal and transverse piezoresistive coefficients, respectively. $\boldsymbol{\sigma}_l$ and $\boldsymbol{\sigma}_t$ are the longitudinal and transverse stress, respectively.

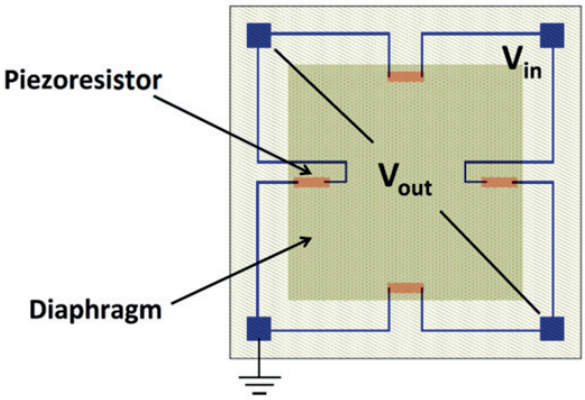

Figure 6: Top view of a piezoresistive pressure sensor diaphragm with piezoresistors.

The piezoresistors on the diaphragm have a finite size and therefore the stress on the piezoresistors must be calculated by averaging the stresses as shown in Eqs. (17) and (18).

$$\sigma_{yave} = \frac{1}{A}\int_y\int_x \sigma_y dxdy \quad (17)$$

$$\sigma_{xave} = \frac{1}{A}\int_y\int_x \sigma_x dxdy \quad (18)$$

where $\boldsymbol{\sigma}_{xave}$ and $\boldsymbol{\sigma}_{yave}$ are the average x- and y-directed stresses at the piezoresistor location, respectively. A is the area of each piezoresistor. Substituting $\boldsymbol{\sigma}_{x\,ave}$ for $\boldsymbol{\sigma}_l$ and the value of $\boldsymbol{\sigma}_{y\,ave}$ for $\boldsymbol{\sigma}_t$ in Eq. (16), we obtain:

$$\frac{\Delta R}{R} = \pi_l \sigma_{xavg} + \pi_t \sigma_{yavg} \quad (19)$$

A computer program is developed using the solution of plate equation and the change in resistance of piezoresistors on the diaphragm. The four piezoresistors are placed at the center of the edges of the diaphragm in order to experience maximum stresses. The program

calculates the stress distribution at the surface of the diaphragm using Eqs. (6) and (7) and the longitudinal and transverse stresses over the piezoresistors are averaged to find the change in resistance of each resistor. The piezoresistors are assumed to be aligned along <110> direction on (100) plane. The piezoresistors are assumed to have p-type doping, for maximum sensitivity [14]. The Wheatstone bridge is provided with an input of 5 V. The sensitivity of the pressure sensor is the relative change in the output voltage per unit change in applied pressure [6]. The pressure vs. output voltage graph is not a straight line and the nonlinearity of the sensor is calculated using an end point straight line [6]. To demonstrate the usage of analytical equations, different sensor structures with diaphragm sizes and thicknesses are chosen as shown in Table 3. A pressure of 10 Bar is applied on each of these models. Four piezoresistors are placed at the edge of the diaphragm with dimensions: 100 µm (length) × 10 µm (width). It is assumed that the contact with the resistor is made at the two ends of the resistor. Usage of analytical solutions for analyzing pressure sensor diaphragms entails that the diaphragm must neither be too thin nor too thick. The reason for the same has been explained in the earlier section. As a thumb rule, for a particular diaphragm size and thickness chosen in Table 3, the diaphragm deflection at full scale pressure is kept between 1/5th and 1/10th of diaphragm thickness. The sensitivity plots of the different models are shown in Fig. 7 and the non-linearity plots is shown in Fig. 8. To find the sensitivity of a particular model, the slope of the curve must be divided by the supply voltage (5 V). The non-linearity of the sensor is the maximum percentage non-linearity for the particular sensor structure. The sensitivity and non-linearity for a particular pressure range can be optimized according to requirement by varying the diaphragm size, diaphragm thickness, piezoresistor dimensions and piezoresistor placement. However, the limitations and conditions required for using analytical solutions as explained earlier must be considered during design optimization.

Table 3: Dimensions for different sensor structures (Pressure – 10 Bar)

Model no.	Diaphragm size (µm × µm)	Diaphragm thickness (µm)
1	600 × 600	15
2	800 × 800	22
3	1000 × 1000	30
4	1200 × 1200	35
5	1400 × 1400	42
6	1600 × 1600	48

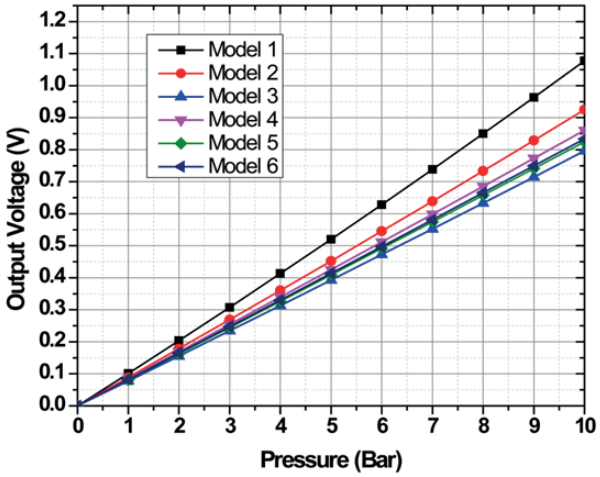

Figure 7: Sensitivity plots for different models.

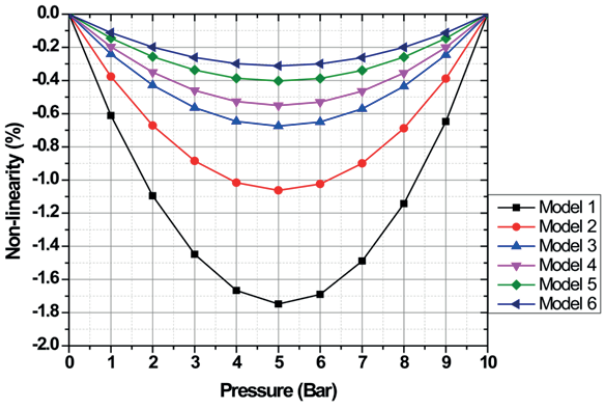

Figure 8: Non-linearity plots for different models.

6 Conclusions

This paper gives a description of the various analytical solutions of plate equation available in literature and delineates the limitation of using these solutions for modeling the diaphragm of a piezoresistive pressure sensor. However, analytical solutions of a plate can be used for obtaining the sensitivity and non-linearity of a pressure microsensor when the diaphragm is neither too thick nor too thin. The various analytical solutions are also compared with FEM solution to obtain the most accurate solution. The method for obtaining the output characteristics of the sensor using analytical equations is also explained. Using the method shown in this paper, analytical solutions can be used for the first level design and optimization of a piezoresistive pressure sensor. This may then be followed up by FEM simulations for the optimized model. Analytical methods help in saving time compared to FEM method.

7 Acknowledgements

Authors would like to acknowledge the generous support of the Director, CSIR-CEERI, Pilani. The authors would also like to thank all the scientific and technical staff of MEMS and Microsensors Group at CSIR-CEERI, Pilani. The financial support by Council of Scientific and Industrial Research (CSIR) through PSC-201: MicroSenSys project is gratefully acknowledged.

8 References

1. N. Yazdi, F. Ayazi, and K. Najafi, "Micromachined inertial sensors," Proc. IEEE, vol. 86, no. 8, pp. 1640–1659, Aug. 1998.
2. W. P. Eaton, and J. H. Smith, "Micromachined pressure sensors: Review and recent developments," Smart Mat. Struc., vol. 6, no. 5, pp. 530–539, Oct. 1997.
3. Y.-H. Zhang, C. Yang, Z.-H. Zhang, H.-W. Lin, L.-T. Liu, and T.-L. Ren, "A novel pressure microsensor with 30-μm-thick diaphragm and meander-shaped piezoresistors partially distributed on high-stress bulk silicon region," IEEE Sensors J., vol. 7, no. 12, pp. 1742-1748, Dec. 2007.
4. M. Olszacki, C. Maj, M. Al-Bahri, P. Pons, and A. Napieralski, "A multi-domain piezoresistive pressure sensor design tool based on analytical models," in Proc. 9th Int. Conf. on Thermal, Mechanical and Multiphysics Simulation and Experiments in Micro-Electronics and Micro-Systems (EuroSimE), April 20-23, 2008, pp. 1-4.
5. D. Maier-Schneider, J. Maibach, and E. Obermeier, "A new analytical solution for the load-deflection of square membranes," J. Microelectromech. Syst., vol. 4, pp. 238–241, 1995.
6. M. Bao, Analysis and Design Principles of MEMS Devices. Amsterdam, The Netherlands: Elsevier, Jun. 10, 2005, pp. 247-303.
7. S. Chen, M.-Q. Zhu, B.-H. Ma, and W.-Z. Yuan, "Design and optimization of micro piezoresistive pressure sensor," in Proc. 3rd IEEE Int. Conf. on Nano/Micro Eng. Molecular Syst., 2008, pp. 351-356.
8. A. L. Herrera-May, B. S. Soto-Cruz, F. López-Huerta, and L. A. Aguilera Cortés, "Electromechanical analysis of a piezoresistive pressure micro-sensor for low-pressure biomedical applications," Revista Mexicana De Física, vol 55, pp. 14-24, 2009.
9. G. Blasquez, Y. Naciri, P. Blondel, N. B. Moussa, and P. Pons, "Static response of miniature capacitive pressure sensor with square or rectangular silicon diaphragm," Rev. Phys. Appl., vol. 22, no. 7, pp. 505-510, 1987.
10. F. Kerrour, and F. Hobar, "A novel numerical approach for the modelling of the square shaped silicon membrane," J. Semicond., Phy., Quantum Electron. and Optoelectron., vol. 9, no.4, pp. 52-57, 2006.
11. S. Timoshenko, and S. Woinowsky-Krieger, Theory of Plates and Shells, 2nd ed. New York: McGraw-Hill, 1959, pp. 79-83.
12. M. A. Hopcroft, W. D. Nix, and T. W. Kenny, "What is the Young's Modulus of Silicon?," J. Microelectomech. Syst., vol. 19, pp. 229-238, 2010.
13. C. S. Smith, "Piezoresistance effect in germanium and silicon," Phys. Rev., vol. 94, pp. 42–49, 1954.
14. Samaun, K. D. Wise, and J. B. Angell, "An IC piezoresistive pressure sensor for biomedical instrumentation," IEEE Trans. Biomed. Engg., vol. BME-20, no. 2, pp.101-109, Mar. 1973.

Arrived: 06. 08. 2014
Accepted: 05. 11. 2014